MCB
Journals.ASM.org

The Arginine Attenuator Peptide Interferes with the Ribosome Peptidyl Transferase Center

Jiajie Wei, Cheng Wu, and Matthew S. Sachs

Department of Biology, Texas A&M University, College Station, Texas, USA

The fungal arginine attenuator peptide (AAP) is encoded by a regulatory upstream open reading frame (uORF). The AAP acts as a nascent peptide within the ribosome tunnel to stall translation in response to arginine (Arg). The effect of AAP and Arg on ribosome peptidyl transferase center (PTC) function was analyzed in *Neurospora crassa* and wheat germ translation extracts using the transfer of nascent AAP to puromycin as an assay. In the presence of a high concentration of Arg, the wild-type AAP inhibited PTC function, but a mutated AAP that lacked stalling activity did not. While AAP of wild-type length was most efficient at stalling ribosomes, based on primer extension inhibition (toeprint) assays and reporter synthesis assays, a window of inhibitory function spanning four residues was observed at the AAP's C terminus. The data indicate that inhibition of PTC function by the AAP in response to Arg is the basis for the AAP's function of stalling ribosomes at the uORF termination codon. Arg could interfere with PTC function by inhibiting peptidyltransferase activity and/or by restricting PTC A-site accessibility. The mode of PTC inhibition appears unusual because neither specific amino acids nor a specific nascent peptide chain length was required for AAP to inhibit PTC function.

Translational control mediated by nascent peptides is demonstrated in mammals, fungi, plants, bacteria, and viruses (25, 28, 30, 40, 43, 46, 62). Among regulatory nascent peptides that control gene expression are some that are encoded by upstream open reading frames (uORFs) in mRNA 5′ leaders. The significance of eukaryotic uORFs is increasingly appreciated (2, 11, 14, 22, 35). Translation of uORFs can reduce translation of downstream ORFs and also decrease mRNA stability. Regulation by eukaryotic uORFs and prokaryotic leader peptides (the designation for prokaryotic uORFs) has consequences for a variety of physiological processes (3, 27).

Regulatory nascent peptides can control translation from within the ribosome tunnel by causing ribosomes to stall. In *Escherichia coli*, tryptophanase expression is controlled in response to tryptophan by the TnaC leader peptide which acts as a ribosome arrest peptide (RAP) during translation termination (13). *E. coli* SecM and *Bacillus subtilis* MifM nascent polypeptides contain domains that interact with the ribosome to cause ribosome arrest during elongation (8, 38, 51, 52). Bacterial *erm* and *cml* operons, which confer resistance to macrolides and to chloramphenicol, respectively, are regulated by nascent leader peptides that function as RAPs when the antibiotics are present (16, 31, 32, 44). A nascent peptide designated MTO1 within the *Arabidopsis thaliana CGS1* coding region causes ribosomes to stall during elongation in response to *S*-adenosyl-L-methionine; the stall induces mRNA degradation (10, 39). In mammals, the uORF-encoded RAP MAGDIS regulates the synthesis of *S*-adenosylmethionine decarboxylase in response to polyamines by stalling ribosomes (45, 48). Expression of the human cytomegalovirus (CMV) gp48 gene is reduced by translation of its uORF2 RAP (29), which causes ribosomes to stall at the uORF2 termination codon (5, 6). Ribosomes synthesizing the uORF-encoded fungal arginine attenuator peptide (AAP) stall at the uORF termination codon in response to a high concentration of arginine (Arg) (17, 19, 26, 53–56, 60).

The regulatory AAP uORF is present in the 5′ leaders of fungal mRNAs specifying the glutamine amidotransferase subunit of Arg-specific carbamoyl phosphate synthetase (26, 57). AAP-mediated stalling in response to Arg results in the reduced synthesis of the first enzyme specific for Arg biosynthesis (15). AAP is the best-understood example of a eukaryotic RAP. *In vivo* studies of the *Neurospora crassa arg-2* mRNA, which encodes the AAP uORF, show that the rate of ARG-2 synthesis is reduced in Arg-supplemented medium (33). Polysome profile analyses show that adding Arg to the growth medium shifts the *N. crassa arg-2* and *Saccharomyces cerevisiae CPA1* transcripts that specify the wild-type (WT) uORF-encoded AAP toward the monosome fraction (20, 34). Furthermore, in *S. cerevisiae*, ribosome stalling at the uORF termination codon triggers degradation of the mRNA through the nonsense-mediated mRNA decay pathway (20). Thus, AAP-mediated ribosome stalling can regulate gene expression in *cis* by reducing translation from a downstream start codon in the mRNA and by reducing the stability of this mRNA.

In vitro experiments have contributed to an understanding of the mechanistic basis of AAP function. Toeprinting (primer extension inhibition), which maps the positions of ribosomes on mRNA, shows that when the AAP functions as a uORF, ribosomes arrested at the AAP termination codon block scanning ribosomes from reaching the downstream initiation codon for the genic ORF (21). AAP can also function as an internal polypeptide domain to cause stalling of ribosomes during elongation (17, 60). AAP causes Arg-regulated stalling of fungal, plant, and animal ribosomes, establishing that the AAP and Arg exploit highly conserved ribosome functions to cause stalling (17). Ribosomal peptidyl trans-

Received 28 January 2012 **Returned for modification** 21 February 2012
Accepted 9 April 2012
Published ahead of print 16 April 2012
Address correspondence to Matthew S. Sachs, msachs@mail.bio.tamu.edu.
Supplemental material for this article may be found at http://mcb.asm.org/.

doi:10.1128/MCB.00136-12

ferase function is a likely target, but this has not yet been directly demonstrated.

Structurally, site-specific photo-cross-linking experiments indicate that Arg alters the conformation of the wild-type AAP relative to the ribosome tunnel (61). In high concentrations of Arg (high Arg), a cross-linker placed at AAP Val-7 reacted relatively less to ribosomal protein L17 and more to ribosomal protein L4. Consistent with these data, visualization of ribosome nascent chain complexes containing AAP in the absence of Arg by cryo-electron microscopy (cryo-EM) also indicates that the AAP interacts with ribosomal proteins L4 and L17 at the ribosome tunnel constriction (1).

A hypothesis to explain Arg-regulated ribosome stalling by AAP is that high Arg stabilizes a conformation of the nascent peptide relative to the ribosome that interferes with PTC function, resulting in ribosome stalling. To test this, we used a puromycin release assay to directly examine how the AAP and Arg affect PTC function. Puromycin is an aminonucleoside antibiotic in which part of the molecule resembles the 3′ end of tyrosyl-tRNA (24). During translation, puromycin enters the PTC A site, and the peptidyl transferase reaction transfers the nascent peptide from tRNA to puromycin. The rate of nascent peptide chain transfer to puromycin thus can be used as an indicator of PTC function (12, 23, 36, 37, 58, 59, 63).

Here, we show that AAP functions with Arg to interfere with the PTC function of *N. crassa* and wheat ribosomes. AAP containing the D12N mutation, which eliminates Arg-induced ribosome stalling, also eliminated Arg's effect on PTC function. Importantly, the AAP interfered with the PTC before full-length AAP was synthesized, but full-length synthesis appeared important for most efficient stalling. These data support a model for AAP function in which the inhibition of PTC function is the basis for the AAP's capacity to stall the ribosome. Unlike many other RAPs, specific features of the AAP near the ribosomal catalytic center appear relatively unimportant for stalling.

MATERIALS AND METHODS

Plasmids. Plasmids containing the coding sequences for wild-type Met_9AAP (pJC102) (where Met_9AAP is an AAP construct with eight additional Met codons at the N terminus of the AAP) (see Fig. S1A in the supplemental material) and D12N Met_9AAP (pJCS102) were constructed as described previously (61). The wild-type AAP sequence was replaced by other sequences by replacing the small AgeI-HindIII restriction fragments with annealed synthetic oligonucleotides by ligation (see Table S1 in the supplemental material). To construct plasmid pJW201 (see Fig. S1B in the supplemental material), which contains the uORF-encoded AAP and a downstream luciferase reporter, synthetic complementary oligonucleotides JW001+ and JW001− (see Table S2 in the supplemental material) were annealed and ligated to gel-purified vector pR301 (18) that had been digested with MluI and NcoI. Mutations were introduced into the AAP coding sequence by replacing the small SpeI-HindIII restriction fragment with annealed synthetic oligonucleotides by ligation (see Table S2 and Fig. S1B). To construct plasmid pJF401 (see Fig. S1C), which contained the AAP fused in frame with a luciferase reporter (AAP-LUC), synthetic complementary oligonucleotides (see Table S3 in the supplemental material) were annealed and ligated to gel-purified vector pJW201 that had been digested with SpeI and BstEII. Mutations were introduced into the AAP coding sequence by replacing the SpeI-BstEII restriction fragment with annealed synthetic oligonucleotides by ligation (see Table S3 and Fig. S1C). Plasmids specifying T7LUC and sea pansy luciferase were described previously (53, 55).

RNA synthesis. Capped and truncated mRNAs encoding nascent peptides were transcribed *in vitro* by T7 RNA polymerase (60) using PCR-generated DNA fragments as templates (primers are listed in Table S4 in the supplemental material). Capped and polyadenylated RNAs were transcribed *in vitro* by T7 RNA polymerase from plasmid DNA templates that were linearized with EcoRI (18). Aliquots of transcribed RNAs were electrophoresed in agarose gels adjacent to nucleic acid standards of known quantity and stained with ethidium bromide. Gel images were obtained by a GE Typhoon Trio+ imager and analyzed by ImageQuantTL to determine the relative amounts of RNA.

Cell-free translation analyses. To visualize peptidyl-tRNA by [^{35}S]Met labeling, *in vitro* translation reactions (20 μl) were programmed with 120 ng of RNA. Either micrococcal nuclease-treated *N. crassa* extracts or micrococcal nuclease-treated wheat germ extracts were used (61). [^{35}S]Met (>1,000 Ci/mmol; MP Biomedicals) was added to reaction mixtures at a final concentration of 0.5 μCi/μl. Arg or Arg analogs were added to reaction mixtures as described in the text. For puromycin release assays, translation reaction mixtures were incubated for 5 min at 26°C, and then puromycin at concentrations indicated in the text was added to reaction mixtures. Samples (5 μl) were taken immediately before the addition of puromycin and at time points following addition as indicated (see, for example, Fig. 1A). Samples were mixed with 5 μl of 2× NuPAGE LDS sample buffer (Invitrogen) and put on ice to stop reactions and then analyzed using 12% NuPAGE gels (Invitrogen) with morpholineethanesulfonic acid (MES) running buffer. The gels were fixed and dried, exposed to phosphor screens overnight, and analyzed with a GE Typhoon Trio+ imager and ImageQuantTL software.

To visualize peptidyl-tRNA by ^{32}P probing, *in vitro* translation reaction mixtures (20 μl) were prepared as described above, except that reaction mixtures contained 20 μM Met and no [^{35}S]Met. Following gel electrophoresis, samples were transferred to Zeta-Probe nylon membranes (Bio-Rad). The procedures for electrophoretic transfer, nucleic acid fixation on the membrane, prehybridization, hybridization with ^{32}P-labeled oligonucleotide, and washing were as described previously (50), except that denatured salmon sperm DNA was not included in the prehybridization and hybridization solutions. After membranes were washed, they were exposed to phosphor screens overnight. The DNA probe (JW02, 5′-GATCCACCCAGGGGTCG-3′), which is the reverse complement to nucleotides (nt) 56 to 72 of *N. crassa* $tRNA^{Arg}$ (CGU) (41), was ^{32}P labeled at its 5′ end as described previously (54).

For luciferase reporter assays, the reaction conditions for *in vitro* translation using *N. crassa* extracts were as described previously (56). Translation reaction mixtures (10 μl) were incubated at 25°C for 30 min, and translation was halted by adding 50 μl of 1.2× passive lysis buffer (Promega). For firefly luciferase activity measurements, equal amounts (12 ng) of mRNA encoding firefly luciferase were used to program extracts; 2.5 ng of synthetic mRNA encoding *Renilla* (sea pansy) luciferase was added to all reaction mixtures to serve as an internal control (53). Firefly and sea pansy luciferase enzyme activities were measured using a Dual-Luciferase Reporter Assay System (Promega) with a Victor 3 Multitask plate reader (Perkin Elmer).

The primer extension inhibition (toeprint) assays were accomplished using ^{32}P-labeled primer ZW4 as described previously (47, 56), except that when cycloheximide (CYH) was added to the reaction mixture after 10 min of translation, reactions were immediately processed to preserve signals from ribosomes stalled at termination codons.

RESULTS

AAP interferes with PTC function in response to Arg. We tested whether the AAP directly interfered with PTC function using puromycin release as an assay (Fig. 1A). Cell-free translation extracts were programmed with truncated synthetic mRNA specifying wild-type or mutated AAPs. Ribosomes that translate the AAP coding sequence are expected to accumulate at the 3′ end of the mRNA with the last codon in the P site. The nascent AAP would

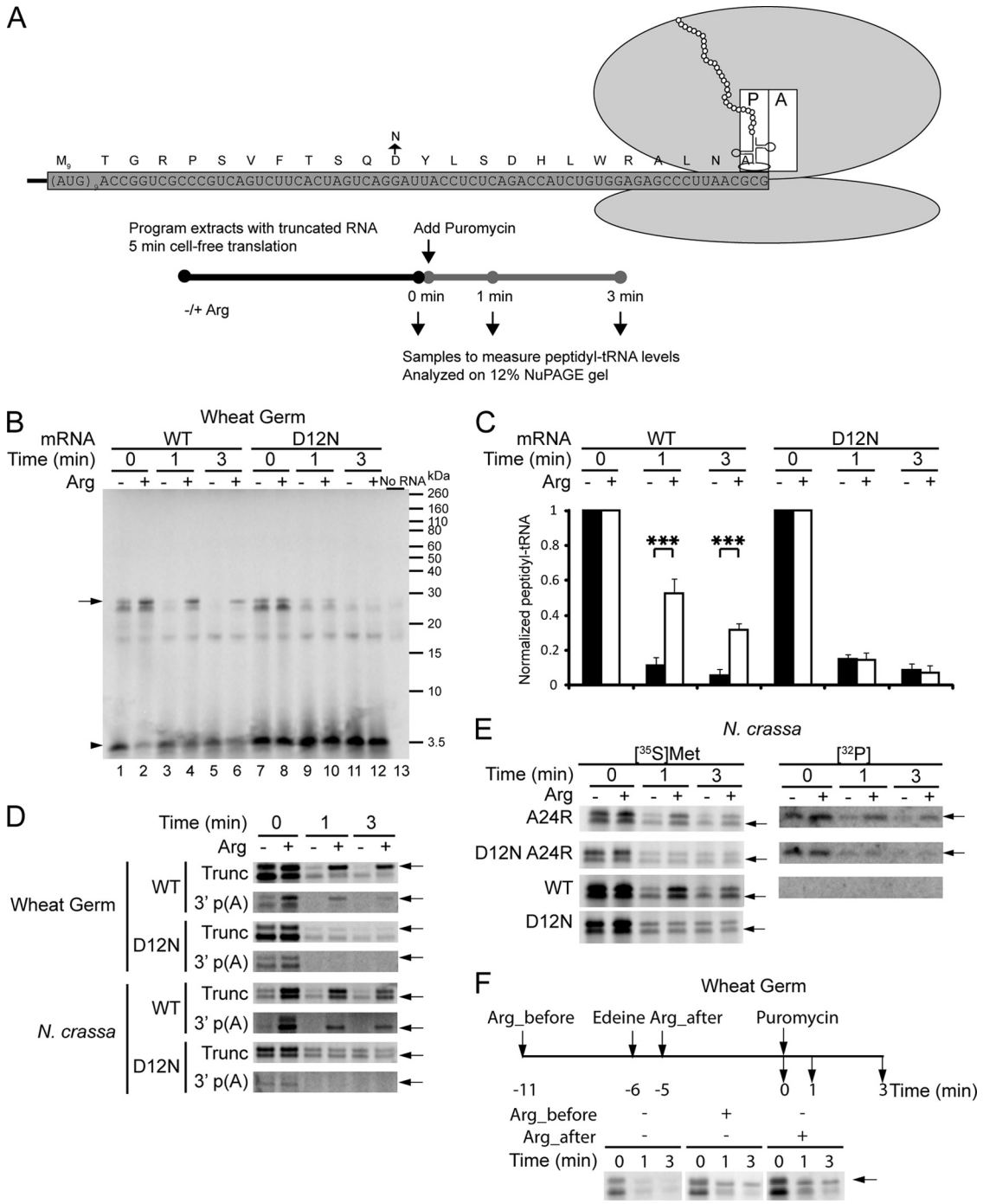

FIG 1 Puromycin release assay to assess the effects of AAP and Arg on PTC function. (A) Synthetic truncated mRNA specifying the *N. crassa* AAP is translated in cell-free systems. Because the mRNA lacks in-frame stop codons, the full-length nascent peptide should remain associated with ribosomes as peptidyl-tRNA with the last encoded amino acid in the ribosome P site. After translation at 26°C for 5 min, puromycin is added to the reaction mixture. Samples are taken immediately before the addition of puromycin (time zero) or at 1 and 3 min following the addition. Translation products are analyzed on 12% NuPAGE gels. Translation reaction mixtures contained either low (−) Arg (20 μM) or high (+) Arg (2 mM). (B) Puromycin release assay to examine the functions of WT and D12N AAPs in wheat germ extract. Translation reaction mixtures contain either low (−) or high (+) Arg. Samples were taken at time zero and at 1 and 3 min after the addition of 1 mM puromycin. Lane 13 represents a control reaction mixture to which no mRNA was added. Arrow, [^{35}S]Met-labeled AAP-tRNA that was resistant to puromycin release in high Arg; arrowhead, [^{35}S]Met-labeled free AAP and AAP-puromycin. (C) Quantification of the puromycin release assay of WT and D12N AAP-tRNAs in wheat germ extract. The signals representing AAP-tRNAs at 1 and 3 min were normalized to the signal at time zero. Mean values and standard deviations from three independent experiments are given (***, $P < 0.001$, Student's *t* test). (D) Puromycin release assay to compare the effect of translating truncated mRNA to mRNA with a 3′ poly(A) tail in wheat germ and *N. crassa* extracts. mRNAs encoding WT and D12N AAPs were used. Samples were taken at time zero and at 1 and 3 min after the addition of 1 mM puromycin (wheat germ extract) or 0.1 mM puromycin (*N. crassa* extract). A representative result of triplicate experiments is shown. Trunc, truncated mRNA; 3′ p(A), mRNA with an intact AAP stop codon and a 3′ poly(A) tail. (E) Puromycin release assay in *N. crassa* extract. Samples were taken at time zero and at 1 and 3 min after the addition of 0.1 mM puromycin. A24R, D12N A24R, WT, and D12N AAPs

thus be in peptidyl-tRNA form at the P site. The AAP is visualized by [^{35}S]Met labeling; eight additional Met residues are encoded at the AAP's N terminus to increase labeling (19). After translation of the RNA for 5 min at 26°C in either low (20 μM) or high (2 mM) Arg concentrations, puromycin is added to the reaction mixtures. Samples are taken immediately before the addition of puromycin (time zero [T_0]) and at 1-min and 3-min time points following puromycin addition (Fig. 1A). The [^{35}S]Met-labeled reaction products are analyzed using 12% NuPAGE gels. AAP-tRNA and AAP released from tRNA can thus be resolved, and the amount of [^{35}S]Met in AAP-tRNA form can be quantified.

The addition of Arg lowered the rate of puromycin-induced release of wild-type (WT) AAP-tRNA in wheat germ extract (Fig. 1B). In a low concentration of Arg (low Arg), WT AAP-tRNA, which migrated with an apparent mass of ≈28 kDa and which was RNase sensitive (see Fig. S2 in the supplemental material), disappeared rapidly following the addition of 1 mM puromycin (Fig. 1B, lanes 3 and 5 versus lane 1; quantification is given in Fig. 1). The decrease in the AAP-tRNA species in response to puromycin was accompanied by an increase in the AAP (mass of ≈3.8 kDa; the AAP is expected to be linked to puromycin, whose mass did not have a detectable impact on the AAPs' migration in this gel system). This indicated that in low Arg, the PTC relatively efficiently transferred the nascent AAP from AAP-tRNA to puromycin. However, in a high concentration of Arg (high Arg), WT AAP-tRNA did not decrease as rapidly in response to puromycin, indicating that Arg interfered with PTC function (Fig. 1B, lanes 4 and 6 versus lane 2; quantification in Fig. 1). The difference in puromycin release rates in low versus high Arg was significant ($P < 0.001$, Student's t test). The WT AAP-tRNA band was stronger, and the free AAP band was weaker in high Arg even before puromycin treatment (Fig. 1B, lane 2 versus lane 1), which is also consistent with Arg having a stabilizing effect on the nascent WT AAP-tRNA in the ribosome. In other words, the increased level of WT AAP-tRNA in the presence of high Arg could reflect reduced spontaneous hydrolysis of the peptidyl-tRNA (42). Asp-12 of AAP is functionally important, and the D12N mutation abolishes AAP-mediated stalling in response to Arg (reference 49 and references therein). For the nonfunctional D12N AAP, AAP-tRNA disappeared rapidly in response to puromycin in both low Arg (Fig. 1B, lanes 9 and 11 versus lane 7; quantification in Fig. 1) and high Arg (Fig. 1B, lanes 10 and 12 versus lane 8; quantification in Fig. 1), indicating that Arg did not affect PTC function when ribosomes contained D12N AAP-tRNA. These data show that the D12N AAP did not inhibit PTC function in response to Arg.

The data in Fig. 1B show AAP-tRNA as a doublet band. This doublet was RNase sensitive (see Fig. S2 in the supplemental material), but only the upper band (arrow) was stabilized for WT AAP in high Arg concentrations. To assess whether the doublet occurred as a consequence of using truncated RNA as a template for translation and to test whether the PTC of *N. crassa* ribosomes is also inhibited by AAP in high Arg, we compared wheat germ and *N. crassa* translation extracts programmed with truncated RNA or poly(A) mRNA (Fig. 1D). The poly(A) mRNA contained an AAP with a termination codon and a 3′ untranslated region (UTR). Overall, the truncated mRNAs encoding the WT AAP and the D12N AAP behaved similarly to the corresponding poly(A) mRNAs in both extracts (Fig. 1D): the WT AAP-tRNA species but not the D12N AAP-tRNA species showed resistance to puromycin release in high Arg. In wheat germ extract, the upper band of the doublet was more resistant to puromycin; in *N. crassa* extract, the lower band was more resistant. The difference between wheat and *N. crassa* extracts could be expected to reflect differences in the tRNAs of these organisms. Furthermore, in extracts programmed with poly(A) RNA, the band that was not stabilized by Arg for WT AAP in response to puromycin was reduced overall. Based on these results and the data described below, this second band might represent ribosomes whose movement is blocked by the ribosome either at the 3′ end of the truncated RNA or at the uORF termination codon. While the identity of this second band has not been elucidated, we confirmed, as shown next, that in *N. crassa* extracts, the puromycin-resistant band (lower band) corresponded to full-length AAP-tRNA.

We examined Arg-specific regulation of AAP-tRNA release both by [^{35}S]Met labeling of the peptide and by ^{32}P probing of the tRNA in *N. crassa* extract. [^{35}S]Met labeling (Fig. 1E) showed that A24R AAP (AAP with a CGU-encoded Arg at its C terminus) functioned similarly to WT AAP (AAP with a GCG-encoded Ala at its C terminus) to inhibit puromycin release in high Arg. D12N A24R AAP and D12N AAP did not respond to Arg (Fig. 1E). Thus, consistent with observations that A24R AAP is functional for stalling (49), the A24R mutation at the C terminus of the AAP did not affect the AAP's ability to regulate PTC function. Next, samples that lacked [^{35}S]Met were probed with a ^{32}P-labeled oligonucleotide, complementary to *N. crassa* tRNA^{Arg} (CGU) (41). The peptidyl-tRNA bands of A24R AAP and D12N A24R AAP but not WT AAP were detected (Fig. 1E), and A24R AAP-tRNA was resistant to puromycin release in high Arg. These data showed that Arg stabilized the functional AAP that was fully synthesized from truncated RNA. AAP-tRNA appeared as a single band by tRNA-probing, not as a doublet, and based on its position relative to polypeptide size markers, this band corresponded to the lower band of the doublet observed by [^{35}S]Met labeling in *N. crassa* extract. We confirmed the specificity of the CGU probe by showing that it did not recognize AAP-tRNA with a C-terminal CGC Arg-codon (see Fig. S3 in the supplemental material).

We next examined the effect on puromycin release of adding high Arg concentrations to reaction mixtures in which full-length AAP was synthesized in low Arg concentrations (Fig. 1F). Previous work indicates that the relative conformation of the AAP changes with respect to the ribosome under these conditions (61). We added edeine, which blocks translation initiation, after 5 min of translation to stop new synthesis of AAP. One minute later, 2 mM Arg was added, and 5 min after that, the puromycin release assay was performed. The results of adding 2 mM Arg after edeine ad-

were analyzed. AAP-tRNA was labeled with [^{35}S]Met (left), or a ^{32}P-labeled tRNA^{Arg} (CGU) probe (right) was used. A representative result of triplicate experiments is shown. (F) Adding Arg after AAP synthesis to assess the regulatory effect on PTC function. The puromycin release assay was performed as shown in the upper panel. After translation in wheat germ for 5 min, edeine was added to block translation initiation. Arg (2 mM) was added either before translation was started or after the addition of edeine. The effects on puromycin-induced release of nascent peptide were compared to a reaction mixture that did not contain high Arg.

dition were similar to those of adding 2 mM Arg at the beginning of translation; in each case, PTC function was inhibited relative to a reaction mixture containing a low concentration of Arg (Fig. 1F). These data indicate that a high concentration of Arg can induce a change in the PTC of ribosomes that have synthesized AAP in low Arg.

Parameters that affect Arg- and AAP-mediated inhibition of PTC function. We next examined effects of different parameters on the efficiency of puromycin release in wheat germ and *N. crassa* extracts. The effects of different puromycin concentrations were tested (see Fig. S4A in the supplemental material). In both extracts, 0.025 mM puromycin appeared sufficient in low Arg to effectively release the nascent AAP from the tRNA at the 3-min time point. In wheat germ extract, varying the concentration of puromycin from 0.025 mM to 1 mM had little impact on Arg's inhibitory effect on puromycin release. However, in *N. crassa* extract, when the concentration of puromycin was greater than 100 μM, we did not observe an effect of Arg, indicating that the kinetics of release were too rapid relative to the time points that were sampled. This difference in sensitivity of puromycin release might be due to differences in the overall sensitivity of these translation extracts to puromycin. The *N. crassa* extract was more sensitive than the wheat germ extract to puromycin, based on the ability to synthesize luciferase in the presence of increasing amounts of puromycin (see Fig. S4B in the supplemental material). We used 1 mM puromycin with wheat germ extract and 0.1 mM puromycin with *N. crassa* extract.

The effect of Arg concentration on puromycin release was tested next (Fig. 2A). We observed increased inhibition of WT AAP-tRNA release as the concentration of Arg increased from 0.25 mM to 2 mM in wheat germ extract. Was this due to nonspecific electrostatic effects of Arg? To test this, we compared the effects of adding either 2 mM Arg or a 2 mM concentration of the stereoisomer D-Arg on puromycin-release. D-Arg, which does not induce stalling (49), also had no discernible impact on puromycin-induced release (Fig. 2B), showing that the effect of Arg on PTC function required L-Arg.

Although D-Arg did not directly induce regulation by the AAP, it was possible that it could competitively inhibit Arg's capacity to induce regulation. We tested this in *N. crassa* extract by analyzing the effects of increasing concentrations of Arg on the synthesis of a firefly luciferase reporter in the presence or absence of 2 mM D-Arg (Fig. 2C). The ability of the uORF-encoded AAP to downregulate firefly luciferase reporter synthesis is a measurement of ribosome stalling at the uORF (55). As observed previously, Arg regulation by AAP was relatively efficient, and addition of Arg at concentrations ranging from 0.25 mM to 2 mM significantly reduced luciferase synthesis ($P < 0.001$, Student's t test). Addition of 2 mM D-Arg as a competitive inhibitor at each of these Arg concentrations did not interfere with regulation. In addition, when D-Arg was added to translation reaction mixtures with 0.5 mM Arg or 2 mM Arg, puromycin-induced release of AAP-tRNA was not affected (Fig. 2D, lanes 6, 9, 15, and 18 versus lanes 5, 8, 14, and 17). Therefore, the effects of Arg on AAP-specific regulation were stereospecific, and the site(s) at which Arg functioned was not blocked by D-Arg.

Arg-regulated stalling by the AAP requires that Arg has a free N terminus (49). An Arg-Gly-Asp (RGD) tripeptide, which can induce AAP-mediated ribosome stalling (49) and induce a change in the AAP's relative conformation in the ribosome (61), also was inhibitory to puromycin release, albeit more weakly than Arg (Fig. 2B). A Gly-Arg-Gly (GRG) tripeptide and Gly-Arg-Gly-Asp (GRGD) tetrapeptide did not inhibit puromycin release (Fig. 2B). These data indicate that the free amino group of Arg is important for the AAP-mediated inhibition of PTC function.

The regulatory functions of extended and shortened AAPs. Toeprinting analyses indicated that Arg-specific ribosome stalling was considerably diminished when the *N. crassa* AAP was shortened by a single residue at its C terminus (18). However, C-terminally shortened AAPs still undergo a change in conformation relative to the ribosome in response to Arg (61). Toeprinting analyses also indicated that AAPs extended at their C termini retain regulatory activity (18). Since puromycin-induced release is a direct assay of PTC function, we used this assay to examine the function of C-terminally extended and shortened AAPs.

Programming wheat germ extracts with truncated mRNAs specifying AAPs ending at Val-25 (AAP_{25}, in which the AAP stop codon is changed to a valine codon), Ala-24 (AAP_{24}, the WT AAP), Asn-23 (AAP_{23}), and Leu-22 (AAP_{22}) showed that each AAP inhibited puromycin-induced release of the nascent chain in a high concentration of Arg (Fig. 3A). However, AAPs ending at Ala-21 (AAP_{21}) or Arg-20 (AAP_{20}) did not inhibit puromycin release (Fig. 3A). These results indicate that AAPs extended by one residue or shortened at the C terminus by one or two residues regulated PTC function in response to Arg, but further shortening eliminated this regulatory function.

We tested whether C-terminally shortened AAPs were capable of regulating translation in response to Arg when encoded as uORFs in the 5′ UTRs of capped and polyadenylated luciferase reporter mRNAs (Fig. 3B). In *N. crassa* extract, the full-length wild-type AAP (AAP_{24}) conferred approximately 5-fold regulation; AAP_{23} and AAP_{22} conferred approximately 2-fold regulation. AAPs truncated further (AAP_{21} and AAP_{20}) showed no regulatory function in response to Arg. Similarly, mRNAs that lacked the uORF-encoded AAP (T7 LUC) or that contained the D12N AAP did not show Arg-regulated synthesis of luciferase (Fig. 3B). These results are consistent with those obtained from the puromycin release assay (Fig. 3A) and indicate that AAPs shortened by one or two residues still confer regulation in response to Arg.

We next directly examined the capacity of these uORF-encoded AAPs to stall ribosomes in *N. crassa* extracts using the toeprinting assay, which shows the positions of ribosomes engaged in the translation of mRNA (Fig. 4C). Cycloheximide (CYH) was added at 0 min (T_0) or 10 min (T_{10}) to increase the signals from ribosomes at translation initiation sites (20). When CYH was added at T_0, both D12N and WT (AAP_{24}) mRNAs showed similar levels of ribosomes at the uORF and luciferase (LUC) initiation codons, either in low or high Arg (Fig. 4C, lanes 5 and 6 and lanes 9 and 10). This is consistent with leaky scanning of ribosomes past the uORF initiation codon (20). When CYH was added after 10 min, an increased toeprint signal that corresponded to ribosomes stalled at the AAP_{24} uORF termination codon and a reduced signal corresponding to ribosomes at the LUC initiation codon were observed in extracts containing high Arg (Fig. 3C, lane 12 versus lane 11). Additional toeprint signals, approximately 30 nt upstream of the toeprints for ribosomes stalled at the termination codon, are interpreted to be ribosomes stalled behind those which are primarily stalled by Arg (53). These differences in signal intensity were not observed for D12N AAP, which lacks regulatory activity (Fig. 3C, lane 8 versus lane 7). This is consistent with

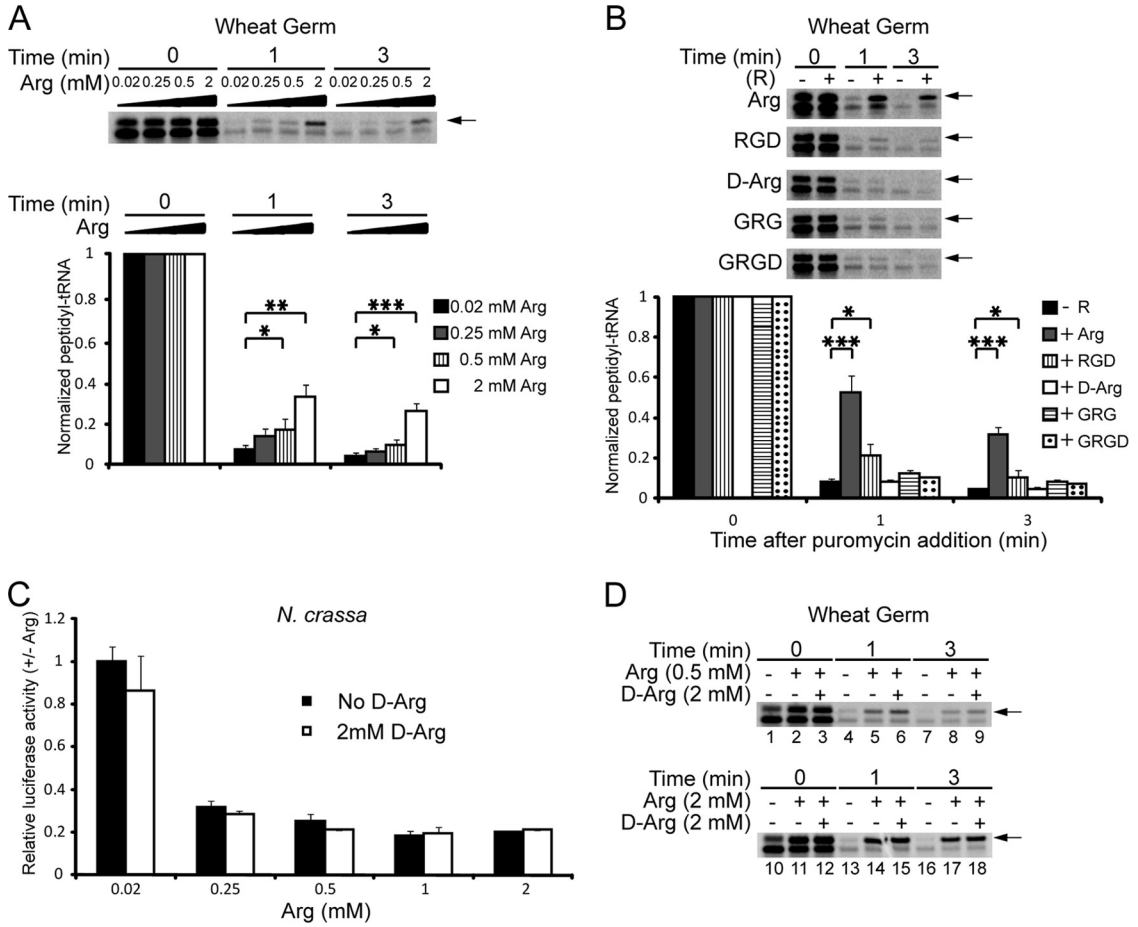

FIG 2 The effects of Arg concentration and Arg analogs on the puromycin release assay. (A) Wheat germ extract supplemented with different concentrations of Arg (0.02, 0.25, 0.5, and 2 mM) was programmed with truncated mRNA specifying WT AAP. Samples were taken at time zero and at 1 and 3 min after the addition of 1 mM puromycin. Arrow, [^{35}S]Met-labeled AAP-tRNA that was resistant to puromycin release in high Arg. In the lower panel, the signals representing peptidyl-tRNAs at 1 and 3 min were normalized to the signal at time zero in different concentrations of Arg. Mean values and standard deviations from three independent translation reactions are shown (*, $P < 0.05$; **, $P < 0.01$; ***, $P < 0.001$, Student's *t* test). (B) The effect of Arg analogs on the puromycin release in wheat germ extract programmed with truncated mRNA encoding WT AAP. −, the translation reaction mixture contained low Arg; +, the translation reaction mixture contained a 2 mM concentration of Arg or of the following Arg analogs as indicated: D-Arg, RGD, GRGD, and GRG. In the lower panel, the signals representing AAP-tRNAs at 1 and 3 min were normalized to the signal at time zero. Mean values and standard deviations from three independent translation reactions are shown (*, $P < 0.05$; ***, $P < 0.001$, Student's *t* test). (C) The effect of Arg concentration on AAP-mediated regulation of luciferase reporter synthesis. Equal amounts of AAP-LUC mRNA were translated in *N. crassa* extract supplemented with 0.02, 0.25, 0.5, 1, or 2 mM Arg in the absence or presence of 2 mM D-Arg. All reaction mixtures contained mRNA for sea pansy luciferase. Firefly luciferase synthesis was first normalized to sea pansy luciferase synthesis. The levels of synthesis are shown relative to the levels of the extract containing 0.02 mM Arg and no D-Arg. Mean values and standard deviations from three independent experiments, each performed in triplicate, are given. (D) The effect of D-Arg on the release of peptidyl-tRNA by puromycin. Samples were taken at time zero and at 1 and 3 min after the addition of 1 mM puromycin to wheat germ extract. D-Arg and Arg were present as indicated. A representative result of triplicate experiments is shown.

ribosomes stalled at the AAP_{24} termination codon acting to block leaky scanning to the downstream LUC initiation codon. As expected, signals corresponding to ribosomes at initiation or termination codons were not observed in toeprint analyses of RNA alone (Fig. 3C, lane 20) or of extract alone (Fig. 3C, lane 19). Importantly, in reaction mixtures incubated for 10 min, stalling occurred at the termination codons for AAP_{23} and AAP_{22} in high Arg but at a reduced level compared to stalling at the termination codon for AAP_{24} (Fig. 3C, lanes 11 to 16). A high concentration of Arg also reduced the signal corresponding to ribosomes at the LUC initiation codon. The AAP_{21} mRNA in parallel reactions showed no effect of Arg on stalling at the uORF termination codon or LUC initiation codon (Fig. 3C, lane 18 versus lane 17). Thus, with respect to the assessed regulatory activity of truncated AAPs, toeprinting and luciferase reporter data were qualitatively similar (Fig. 3B). The toeprinting signal showed ribosomes stalled with the stop codon in the A site, indicating that the translocation reaction, which transferred the peptidyl-tRNA from the A site to the P site, had occurred in the stalled ribosomes (see Fig. 6).

The observations that truncated AAPs interfered with PTC function suggested that the AAP could inhibit the PTC prior to its complete synthesis. We directly examined this possibility in *N. crassa* extract using $tRNA^{Arg}$ probing. Arg (CGU) codons were strategically placed in mRNAs specifying different truncated AAPs. As expected, when the last codon was Arg (CGU), L22R AAP_{22}, N23R AAP_{23}, A24R AAP_{24}, and *25R AAP_{25} (which has

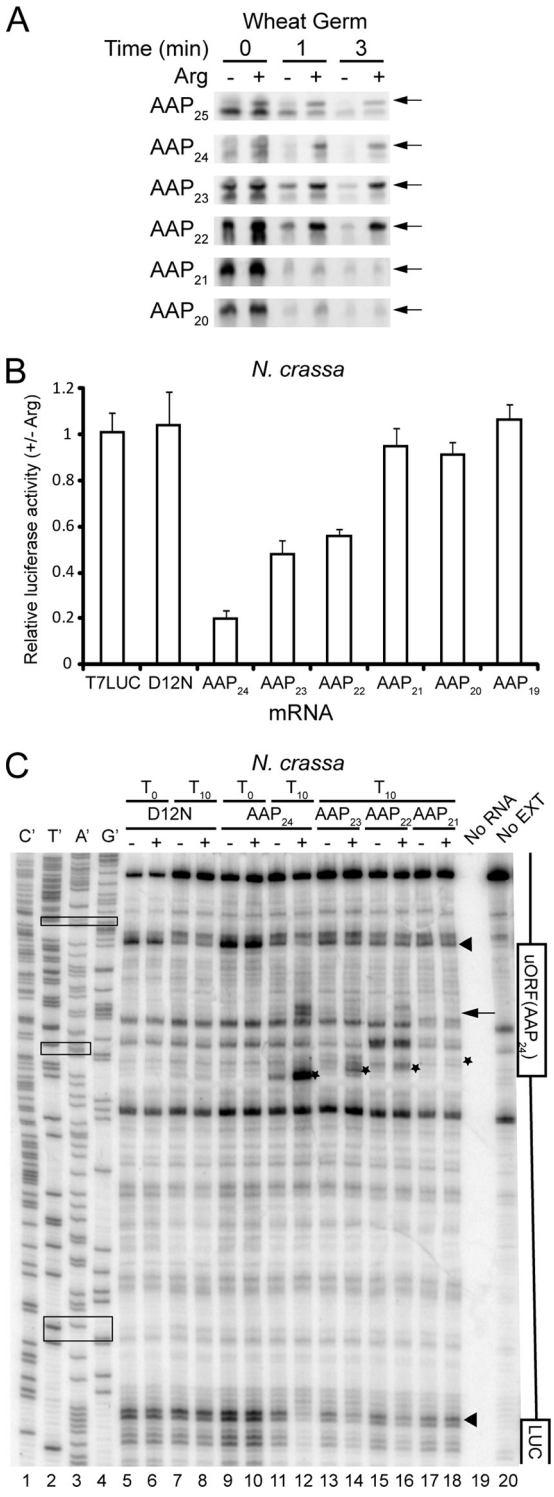

FIG 3 The effects of truncating AAP on Arg-specific translational control. (A) The effect of AAP truncation or extension on puromycin release in wheat germ extract. Samples were taken at time zero and at 1 and 3 min after the addition of 1 mM puromycin. Translation reactions were performed in low (−) or high (+) Arg. For the truncated AAP mRNAs used in these experiments, the numbers in subscripts indicate the length of the AAP (e.g., AAP_{24} indicates that AAP was truncated after position 24). AAP_{25} changes the wild-type stop codon to a valine codon. A representative result of triplicate experiments is shown. Arrows, positions of [^{35}S]Met-labeled AAP-tRNA that showed resistance to puromycin-release in high Arg. (B) The regulatory effects of wild-type and C-terminally truncated AAPs positioned as uORFs in a capped and polyadenylated luciferase reporter. uORFs were created with stop codons at AAP positions 20 to 25 as indicated (e.g., AAP_{24} contains a stop codon at position 25). Equal amounts of each mRNA were translated in *N. crassa* extract containing low or high Arg. As controls, equal amounts of mRNA encoding firefly LUC reporter only (T7 LUC) or mRNA containing the D12N AAP uORF were translated in parallel. All reaction mixtures contained mRNA for sea pansy luciferase to serve as an internal control for translation. Firefly luciferase synthesis was normalized to sea pansy luciferase synthesis, and then luciferase synthesis in high Arg was calculated relative to synthesis in low Arg. Mean values and standard deviations from three independent experiments, each performed in triplicate, are given. (C) Toeprint analysis to assess Arg regulation by WT, D12N, and truncated AAPs. *N. crassa* extract was programmed with equal amounts (60 ng) of mRNA specifying D12N, AAP_{24} (WT), AAP_{23}, AAP_{22}, or AAP_{21} in the 5′ leader. mRNAs were those used for luciferase measurements in panel B. Cycloheximide was added either prior to incubation (T_0) or after 10 min of incubation (T_{10}). Radiolabeled primer ZW4 was used for primer extension analysis and for sequencing the AAP_{24} template (lanes 1 to 4). The nucleotide complementary to the dideoxynucleotide added to each sequencing reaction for the AAP_{24} template is indicated above the corresponding lane so that the sequence of the template can be directly deduced. Asterisks, toeprint products corresponding to ribosomes stalled at the termination codon of AAP; arrowheads, toeprint products corresponding to ribosomes bound at the initiation codons; arrow, toeprint product corresponding to ribosomes stalled approximately 30 nt upstream of those stalled by Arg at the termination codon. Boxes (top to bottom): AAP initiation codon, AAP termination codon, and LUC initiation codon. No EXT, RNA without extract; no RNA, extract without RNA.

the AAP stop codon replaced with the Arg (CGU) codon) all showed regulation in response to Arg based on both [^{35}S]Met and $tRNA^{Arg}$ probing, while A21R AAP_{21} showed no regulation by either measurement (Fig. 4A). These data are consistent with the results obtained for wheat germ extract using [^{35}S]Met labeling (Fig. 3A). In parallel experiments we observed that for truncated mRNA encoding L22R AAP_{24} or N23R AAP_{24}, AAP-$tRNA^{Arg}$ was detected and was resistant to puromycin release in high Arg but not low Arg. These data indicate that Arg regulation of PTC function occurred prior to full synthesis of the AAP. This was not the case for A21R AAP_{24}, which showed regulation by [^{35}S]Met labeling but for which $tRNA^{Arg}$ was not detected (Fig. 4A). This indicated that translation proceeded efficiently past codon 21 and that a regulatory "window" in which Arg could affect the PTC spanned from codon 22 to codon 25 of the AAP.

Interestingly, the peptidyl-tRNA of D12N N23R AAP_{24} was detected by the $tRNA^{Arg}$ probe (Fig. 4A), indicating that translation was slowed prior to the complete synthesis of this AAP. This suggested that, independent of the capacity of the AAP to elicit Arg-regulated stalling, slowing occurs near the AAP C terminus. This could reflect a general inability of the translation system to decode truncated RNA, or it could reflect intrinsic stalling activity of the AAP that was independent of Arg regulation (e.g., that occurred in the presence of the D12N mutation which eliminates regulation). To examine this, we made a construct specifying a frameshift AAP (FS AAP) in which only residues 1 to 3 and 23 to 24 were identical to those in the AAP (Fig. 4B). An Arg (CGU) codon was placed at residue 22, 23, or 24 of WT, D12N, and FS AAPs. Intrinsic stalling activity was measured by translation of equal amounts of each RNA in a low concentration of Arg (Fig. 4B, lower panel) followed by Northern analysis to detect peptidyl-tRNA (Fig. 4B, upper panel). As expected for ribosome nascent chain complex formation on truncated RNA, each mRNA showed a strong signal when the Arg codon was the final codon (AAP

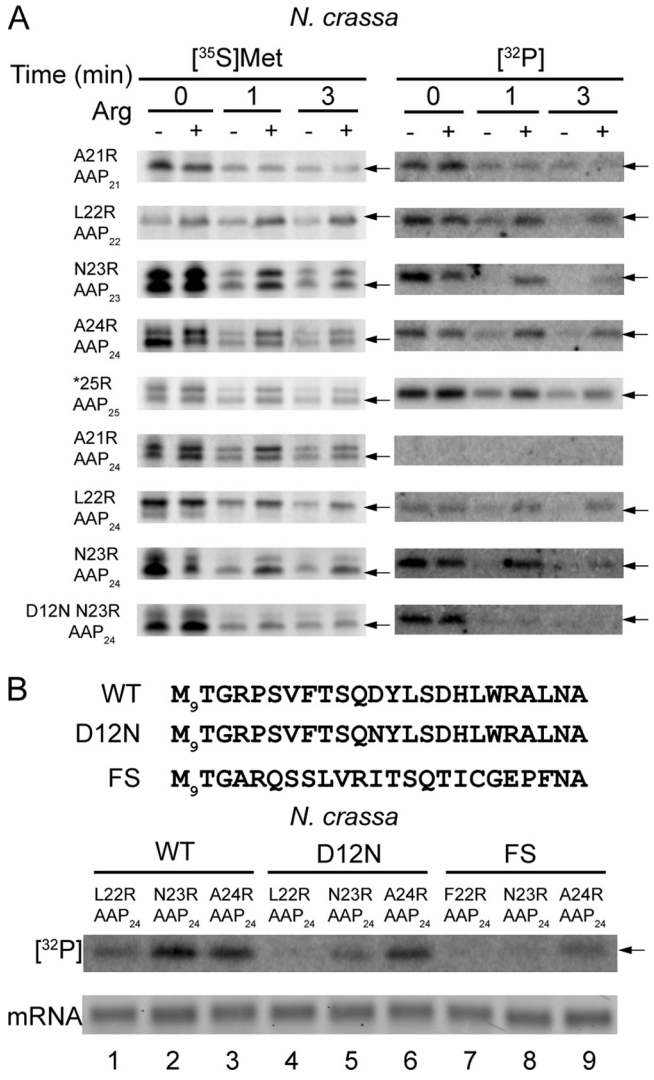

FIG 4 Ribosome stalling prior to complete AAP synthesis. (A) A21R, L22R, N23R, A24R, and *25R indicate that the original codons at AAP positions 21, 22, 23, 24, or 25 were changed, respectively, to CGU Arg codons. AAP_{25}, AAP_{24}, AAP_{23}, AAP_{22}, and AAP_{21} indicate that AAP was truncated after position 25, 24, 23, 22, or 21. *N. crassa* extracts were programmed with the indicated RNAs in either a low (−) or high (+) concentration of Arg. Samples were taken at time zero and at 1 and 3 min after the addition of 0.1 mM puromycin. Arrows indicate the position of peptidyl-tRNA. AAP-tRNA was labeled with [^{35}S]Met (left), or a ^{32}P-labeled $tRNA^{Arg}$ (CGU) probe was used (right). (B) Truncated mRNAs encoding WT AAP, D12N AAP, or frameshift (FS) AAPs, which contained Arg (CGU) codons at the indicated positions, were translated in *N. crassa* extract for 10 min at 26°C. In the upper panel, peptidyl-tRNA (arrow) was detected with ^{32}P-labeled $tRNA^{Arg}$ (CGU) probe. The lower panel shows a gel analysis to establish that similar amounts of input mRNAs were used in the translation reactions shown in the upper panel.

codon 24) of the truncated RNA (Fig. 4B, lanes 3, 6, and 9). When the Arg codon was at AAP codon 22 or codon 23, stronger signals were detected for WT and D12N AAPs than for the FS AAP (Fig. 4B, lanes 2 and 5 versus lane 8 and lanes 1 and 4 versus lane 7), with WT AAP showing the strongest signals overall. These data showed that WT and D12N AAPs exhibited greater intrinsic stalling activity than FS AAP and indicate that evolutionarily conserved elements in the AAP contribute to intrinsic stalling activity even in the absence of Arg-stimulated stalling activity.

A question that arises is whether the presence of novel Arg codons in the AAP coding sequence fortuitously creates new sites for ribosome stalling within the AAP. If this were so, then this could account for the detection of internal stall sites with $tRNA^{Arg}$ probe. We tested this by making constructs in which the AAP was fused in frame with the luciferase coding region. In such constructs, for the wild-type AAP, the primary stalling signals observed by toeprinting are in the region downstream of AAP codon 24 (17, 18, 53). We used toeprinting to analyze ribosome stalling in constructs (see Fig. S1C and Fig. S5 in the supplemental material) that contained wild-type AAP sequence or contained mutations D12N, A21R, L22R, N23R, A24R, or *25R (the latter representing an additional codon in the construct). In each construct, except for the D12N AAP, increased stalling corresponding to ribosomes downstream of codon 24 was observed (see Fig. S5). Additional Arg-regulated stall sites in the AAP coding region approximately 30 nt upstream could be attributed to ribosomes stalled behind those primarily stalled by Arg. Importantly, no additional toeprint signals corresponding to ribosomes stalled at internal positions in the AAPs containing A21R, L22R, N23R, and A24R mutations were observed; thus, these Arg codons did not create new stalling sites.

The effects of other RAPs on peptidyl transferase function. We compared the function of the *S. cerevisiae* AAP (AAP_{Sc}) to the *N. crassa* AAP (AAP_{Nc}) using wheat germ extracts (Fig. 5A and B). In low Arg, both WT AAP_{Sc}-tRNA and WT AAP_{Nc}-tRNA disappeared rapidly following the addition of puromycin. In high Arg, for both WT AAP_{Sc}-tRNA and WT AAP_{Nc}-tRNA, the rates of peptidyl-tRNA disappearance were lower, suggesting that AAP_{Sc} functioned similarly to AAP_{Nc} to inhibit PTC function in response to Arg. Synthesis of cytomegalovirus gp48 is inhibited by translation of a 22-codon uORF (gp48 uORF2); the gp48 uORF2 nascent peptide stalls ribosomes at the uORF2 termination codon (5). gp48 uORF2 was translated in wheat germ extract, and its effects on the PTC were tested using the puromycin release assay (Fig. 5C). WT gp48 uORF2-tRNA did not disappear rapidly following the addition of puromycin (Fig. 5C, lanes 2 and 3 versus lane 1), indicating that WT gp48 uORF2 inhibited PTC function. However, in striking contrast, for the nonfunctional gp48 uORF2 containing the P22A mutation, uORF2-tRNA was released rapidly by puromycin (Fig. 5C, lanes 5 and 6 versus lane 4). Thus, in contrast to results with the AAP, where the identity of the C-terminal amino acid had little impact on inhibition of puromycin release, gp48 uORF2 Pro-22 was crucial for this function. The inhibition of nascent chain release by AAP in high Arg and gp48 uORF2 was directly compared for an extended period of incubation (up to 30 min) in the presence of puromycin. The gp48 uORF2 was more inhibitory than the AAP (see Fig. S6 in the supplemental material). These analyses of gp48 uORF2 indicate an effect of this RAP on the PTC beyond its known effect on inhibiting the function of eukaryotic release factor 1 (eRF1) (29). Preparation of samples for cryo-EM studies by other investigators also indicated that the gp48 uORF2-induced ribosome stall was highly stable (1). However, the possibility that the gp48 uORF2-tRNA is released from the P site but remains associated with ribosomes is another potential explanation for the observed resistance of gp48 uORF2-tRNA to cleavage by puromycin (7).

One difference between gp48 uORF2 and AAP is that gp48 uORF2 ends with a Pro residue, and the presence of a Pro residue in the ribosome P site has been associated with reduced reactivity

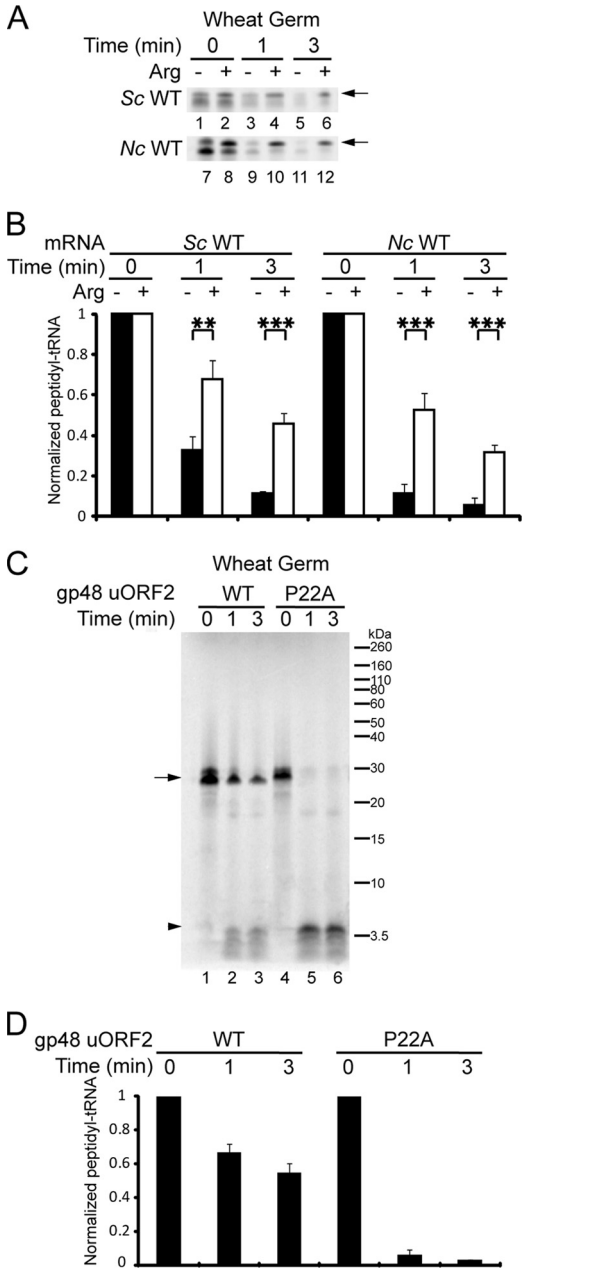

FIG 5 The *S. cerevisiae* AAP and CMV gp48 uORF2 peptide interfere with puromycin release. (A) Truncated mRNAs specifying *S. cerevisiae* (*Sc*) WT AAP and *N. crassa* (*Nc*) WT AAP were translated in wheat germ extract. Samples were taken at time zero and at 1 and 3 min after the addition of 1 mM puromycin. Translation reaction mixtures contained low (−) or high (+) Arg. Arrows, [^{35}S]Met-labeled AAP-tRNA. (B) Quantification of puromycin release assay of AAP_{Sc}-tRNA and AAP_{Nc}-tRNA in wheat germ extract. The signals representing peptidyl-tRNAs at 1 and 3 min were normalized to the signal at time zero. Mean values and standard deviations from three independent translation reactions are given (**, $P < 0.01$; ***, $P < 0.001$, Student's *t* test). (C) The effect of CMV gp48 uORF2 on peptidyl-tRNA release by puromycin. WT gp48 uORF2 peptide and the nonfunctional mutated P22A gp48 uORF2 were tested in wheat germ extract. Samples were taken at time zero and at 1 and 3 min after the addition of 1 mM puromycin. Arrow, [^{35}S]Met-labeled uORF2-tRNA; arrowhead, [^{35}S]Met-labeled free uORF2 and uORF2-puromycin. (D) The signals representing gp48 uORF2-tRNAs at 1 and 3 min were normalized to the signal at time zero. Mean values and standard deviations from three independent translation reactions are given.

toward puromycin (36). We tested the A24P AAP and D12N A24P AAP in the puromycin release assay (see Fig. S6 in the supplemental material). The AAP A24P mutation did not decrease reactivity to puromycin in either the wild-type or D12N AAP context.

DISCUSSION

The nascent AAP interferes with PTC function in the presence of high Arg. Arg-regulated inhibition of PTC function was observed for full-length AAP, for AAP extended by one amino acid at its C terminus (AAP_{25}), and for AAP truncated by one or two amino acids at its C terminus (AAP_{23} or AAP_{22}, respectively) (Fig. 3A, 4A, and 5A). These truncated AAPs, like the full-length AAP, caused regulatory ribosome stalling in response to Arg, albeit with reduced efficiency (Fig. 3B and C). Analyses of tRNA identity also showed that the AAP regulated PTC function prior to its complete synthesis. These results demonstrate that the AAP has the unusual property of interfering with the PTC across a window spanning at least four consecutive codons (AAP codons 22 to 25). We also obtained data indicating that both wild-type AAP and D12N AAP (which lacks regulatory function) had higher intrinsic stalling activity than a frame-shifted peptide. Thus, the AAP appears to have intrinsic stalling activity detectable even in the absence of Arg-regulated stalling.

Ribosomes containing AAP_{24} synthesized in a low concentration of Arg but then subsequently incubated with high Arg show a change in the relative conformation of the AAP with respect to the ribosome (61) and a reduction in PTC function (Fig. 1F). These data support the idea that the Arg-induced change in relative conformation of AAP with respect to the ribosome is necessary to provide the capacity for AAP to interfere with the PTC.

Why does the full-length AAP stall ribosomes more efficiently than AAPs truncated at their C termini? It is not the absolute length of the nascent AAP because while C-terminal truncations AAP_{23} and AAP_{22} reduced the efficiency of ribosome stalling based on reporter synthesis and toeprint assays (Fig. 3B and C), N-terminal truncations yielding even shorter AAPs do not (18). Possibly, in high Arg, when the ribosome translating AAP_{22} or AAP_{23} is stalled because the ribosome has reached the 3′ end of a truncated mRNA, AAP_{22} or AAP_{23} nascent peptides have sufficient opportunity to obtain proper register with respect to the ribosome so that, like AAP_{24}, they can interfere with PTC function. Important in this regard, the relative conformations of each of these C-terminally truncated AAPs also change with respect to the ribosome in response to Arg (61). However, if the mRNA extends past codon 22 or codon 23 because AAP_{22} and AAP_{23} might not adapt or maintain register as efficiently as AAP_{24}, the ribosome translates past codon 22 and codon 23. There is some stalling of ribosomes that are engaged in elongation at these codons, however, as determined by the detection of stabilized AAP-$tRNA^{Arg}$ for L22R AAP_{24} and N23R AAP_{24} (Fig. 4). In contrast, AAP_{21}, which undergoes an Arg-dependent conformational change with respect to the ribosome (61), cannot find the proper register to interfere with the PTC (Fig. 3 and 4). These data suggest a model for AAP-mediated stalling in response to Arg in which the AAP undergoes a change in relative conformation with respect to the ribosome, and this altered conformation must be in proper register with the ribosome to efficiently interfere with PTC function. In this model, there is a window of AAP chain lengths for which AAP can find the register (with respect to the ribosome and possibly with respect to Arg), with the wild-type AAP length being

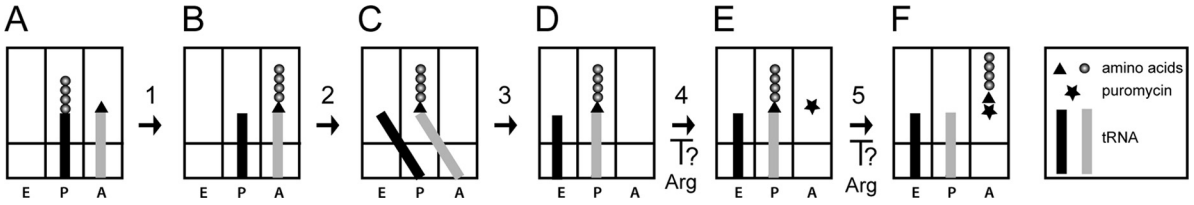

FIG 6 Schematic representation of PTC activity and potential steps affected by the AAP and Arg. (A) The peptidyl-tRNA and aminoacyl-tRNA are in the P and the A sites, respectively, of the peptidyl transferase center of the ribosome. (B) Immediately after peptide bond formation (step 1), a peptidyl-tRNA is in the A site, and an uncharged tRNA is in the P site. (C) The aminoacyl end of the tRNA moves to the P site (step 2), resulting in peptidyl-tRNA in a P/A hybrid site and uncharged tRNA in an E/P hybrid site. (D) The peptidyl-tRNA translocates to the P/P site, and deacylated tRNA translocates to the E/E site (step 3), together with the movement of the associated mRNA by one codon. (E) Puromycin can enter an empty A site as depicted (step 4). (F) The peptidyl transferase reaction transfers the peptide from peptidyl-tRNA to puromycin, resulting in release of the nascent peptide from tRNA (step 5). Symbols are as explained on the figure. Steps 4 and 5 are potentially inhibited by AAP and Arg as indicated (see the text).

most efficient at achieving and/or maintaining this proper register. Consistent with this idea, of 120 uORF-encoded AAPs identified by evolutionary conservation, the C-terminal regions of 119 are at least as long as the *N. crassa* AAP C terminus, and none is more than two residues longer (49).

How is PTC function affected by AAP and Arg to inhibit the function of puromycin? There are at least several ways that access of puromycin to the ribosome A site could be restricted. There could be failure of translocation (Fig. 6, steps 2 and 3), or the structure of the ribosome could be altered such that access to the empty A site is blocked (Fig. 6D, step 4). Alternatively, puromycin could enter the ribosome A site (Fig. 6E), but the peptidyl transferase reaction is inhibited (Fig. 6, step 5). Toeprint analyses of mRNAs on which the AAP stalls ribosomes at its termination codon show that the termination codon is in the A site, indicating that stalling occurs with a configuration of the ribosome depicted in Fig. 6D. Furthermore, AAP can be fully synthesized in low Arg and still interfere with PTC function when Arg is subsequently added (Fig. 1F). These data indicate that Arg's inhibitory effect on PTC function occurs after translocation (after step 3 in Fig. 6). Thus, the relative conformation of the AAP in the ribosome in high Arg could restrict access to the empty A site (Fig. 6, step 4) and/or could interfere with the peptidyl transferase reaction (Fig. 6, step 5). The cryo-EM model of the wheat ribosome containing AAP in the absence of Arg raises the possibility that an altered position of ribosomal protein L10e could be responsible for inhibiting PTC function (1).

Unlike many other RAPs, specific residues of the AAP are not required at or near the PTC for the AAP to cause ribosome arrest. For example, the C-terminal Pro-22 of CMV uORF2 is crucial for stalling (4) and for inhibiting PTC function, based on the puromycin release assay (Fig. 5B). SecM, MifM, TnaC, and ErmAL1 each require specific amino acids at the PTC for stalling to occur (9, 23, 37, 44). ErmCL, ErmAL1, and SecM each also require nearby amino acids (−2 relative to the nascent peptide C terminus) for stalling to occur (44, 63). In contrast, AAP residues 9 to 20 are sufficient to confer regulatory function; moreover, AAP residues 21 to 24 can all be replaced with Ala, and AAP function is retained (49). Furthermore, the evolutionary conservation of residues of the AAP beyond Arg-20 is relatively low.

In summary, we show here that the AAP interferes directly with PTC function in response to Arg. The AAP is an evolutionarily conserved, uORF-encoded regulatory peptide, and there is expanding appreciation of the wider roles for uORFs in controlling gene expression. The AAP represents an unusual example of nascent peptide control of ribosome activity because there is no evident requirement for specific nascent peptide residues to be at or near the PTC for stalling to occur. The AAP stalls ribosomes from fungal, plant, and mammalian sources and thus must exert a regulatory effect through conserved regions of the eukaryotic ribosome. Understanding the function of the AAP provides a basis for gaining insight into fundamental processes by which nascent peptides and metabolites regulate gene expression.

ACKNOWLEDGMENTS

This work was supported by a National Institutes of Health grant to M.S.S. (R01 GM 47498).

We thank Ivaylo Ivanov, Luis Rogelio Cruz-Vera, and Charles Yanofsky for helpful discussion and critical reading of the manuscript.

REFERENCES

1. **Bhushan S, et al.** 2010. Structural basis for translational stalling by human cytomegalovirus and fungal arginine attenuator peptide. Mol. Cell **40**: 138–146.
2. **Brar GA, et al.** 2012. High-resolution view of the yeast meiotic program revealed by ribosome profiling. Science **335**:552–557.
3. **Calvo SE, Pagliarini DJ, Mootha VK.** 2009. Upstream open reading frames cause widespread reduction of protein expression and are polymorphic among humans. Proc. Natl. Acad. Sci. U. S. A. **106**:7507–7512.
4. **Cao J, Geballe AP.** 1996. Coding sequence-dependent ribosomal arrest at termination of translation. Mol. Cell. Biol. **16**:603–608.
5. **Cao J, Geballe AP.** 1996. Inhibition of nascent-peptide release at translation termination. Mol. Cell. Biol. **16**:7109–7114.
6. **Cao J, Geballe AP.** 1994. Mutational analysis of the translational signal in the human cytomegalovirus gpUL4 (gp48) transcript leader by retroviral infection. Virology **205**:151–160.
7. **Cao J, Geballe AP.** 1998. Ribosomal release without peptidyl tRNA hydrolysis at translation termination in a eukaryotic system. RNA **4**:181–188.
8. **Chiba S, et al.** 2011. Recruitment of a species-specific translational arrest module to monitor different cellular processes. Proc. Natl. Acad. Sci. U. S. A. **108**:6073–6078.
9. **Chiba S, Lamsa A, Pogliano K.** 2009. A ribosome-nascent chain sensor of membrane protein biogenesis in *Bacillus subtilis*. EMBO J. **28**:3461–3475.
10. **Chiba Y, et al.** 2003. *S*-Adenosyl-L-methionine is an effector in the post-transcriptional autoregulation of the cystathionine gamma-synthase gene in *Arabidopsis*. Proc. Natl. Acad. Sci. U. S. A. **100**:10225–10230.
11. **Churbanov A, Rogozin IB, Babenko VN, Ali H, Koonin EV.** 2005. Evolutionary conservation suggests a regulatory function of AUG triplets in 5′-UTRs of eukaryotic genes. Nucleic Acids Res. **33**:5512–5520.
12. **Cruz-Vera LR, Gong M, Yanofsky C.** 2006. Changes produced by bound tryptophan in the ribosome peptidyl transferase center in response to TnaC, a nascent leader peptide. Proc. Natl. Acad. Sci. U. S. A. **103**:3598–3603.
13. **Cruz-Vera LR, Rajagopal S, Squires C, Yanofsky C.** 2005. Features of ribosome-peptidyl-tRNA interactions essential for tryptophan induction of *tna* operon expression. Mol. Cell **19**:333–343.

14. **Cruz-Vera LR, Sachs MS, Squires CL, Yanofsky C.** 2011. Nascent polypeptide sequences that influence ribosome function. Curr. Opin. Microbiol. **14**:160–166.
15. **Davis RL.** 1996. Polyamines in fungi, p 347–356. *In* Brambl R, Marzluf G A (ed), The mycota: biochemistry and molecular biology, vol. 3. Springer-Verlag, Heidelberg, Germany.
16. **Dubnau D.** 1985. Induction of ermC requires translation of the leader peptide. EMBO J. **4**:533–537.
17. **Fang P, Spevak CC, Wu C, Sachs MS.** 2004. A nascent polypeptide domain that can regulate translation elongation. Proc. Natl. Acad. Sci. U. S. A. **101**:4059–4064.
18. **Fang P, Wang Z, Sachs MS.** 2000. Evolutionarily conserved features of the arginine attenuator peptide provide the necessary requirements for its function in translational regulation. J. Biol. Chem. **275**:26710–26719.
19. **Fang P, Wu C, Sachs MS.** 2002. *Neurospora crassa* supersuppressor mutants are amber codon-specific. Fungal Genet. Biol. **36**:167–175.
20. **Gaba A, Jacobson A, Sachs MS.** 2005. Ribosome occupancy of the yeast *CPA1* upstream open reading frame termination codon modulates nonsense-mediated mRNA decay. Mol. Cell **20**:449–460.
21. **Gaba A, Wang Z, Krishnamoorthy T, Hinnebusch AG, Sachs MS.** 2001. Physical evidence for distinct mechanisms of translational control by upstream open reading frames. EMBO J. **20**:6453–6463.
22. **Galagan JE, et al.** 2005. Sequencing of *Aspergillus nidulans* and comparative analysis with *A. fumigatus* and *A. oryzae*. Nature **438**:1105–1115.
23. **Gong F, Ito K, Nakamura Y, Yanofsky C.** 2001. The mechanism of tryptophan induction of tryptophanase operon expression: tryptophan inhibits release factor-mediated cleavage of TnaC-peptidyl-tRNAPro. Proc. Natl. Acad. Sci. U. S. A. **98**:8997–9001.
24. **Hansen JL, Moore PB, Steitz TA.** 2003. Structures of five antibiotics bound at the peptidyl transferase center of the large ribosomal subunit. J. Mol. Biol. **330**:1061–1075.
25. **Hood HM, Neafsey DE, Galagan J, Sachs MS.** 2009. Evolutionary roles of upstream open reading frames in mediating gene regulation in fungi. Annu. Rev. Microbiol. **63**:385–409.
26. **Hood HM, Spevak CC, Sachs MS.** 2007. Evolutionary changes in the fungal carbamoyl-phosphate synthetase small subunit gene and its associated upstream open reading frame. Fungal Genet. Biol. **44**:93–104.
27. **Iacono M, Mignone F, Pesole G.** 2005. uAUG and uORFs in human and rodent 5′ untranslated mRNAs. Gene **349**:97–105.
28. **Ito K, Chiba S, Pogliano K.** 2010. Divergent stalling sequences sense and control cellular physiology. Biochem. Biophys. Res. Commun. **393**:1–5.
29. **Janzen DM, Frolova L, Geballe AP.** 2002. Inhibition of translation termination mediated by an interaction of eukaryotic release factor 1 with a nascent peptidyl-tRNA. Mol. Cell. Biol. **22**:8562–8570.
30. **Kurian L, Palanimurugan R, Godderz D, Dohmen RJ.** 2011. Polyamine sensing by nascent ornithine decarboxylase antizyme stimulates decoding of its mRNA. Nature **477**:490–494.
31. **Lawrence MG, Lindahl L, Zengel JM.** 2008. Effects on translation pausing of alterations in protein and RNA components of the ribosome exit tunnel. J. Bacteriol. **190**:5862–5869.
32. **Lovett PS.** 1996. Translation attenuation regulation of chloramphenicol resistance in bacteria—a review. Gene **179**:157–162.
33. **Luo Z, Freitag M, Sachs MS.** 1995. Translational regulation in response to changes in amino acid availability in *Neurospora crassa*. Mol. Cell. Biol. **15**:5235–5245.
34. **Luo Z, Sachs MS.** 1996. Role of an upstream open reading frame in mediating arginine-specific translational control in *Neurospora crassa*. J. Bacteriol. **178**:2172–2177.
35. **Morris DR, Geballe AP.** 2000. Upstream open reading frames as regulators of mRNA translation. Mol. Cell. Biol. **20**:8635–8642.
36. **Muto H, Ito K.** 2008. Peptidyl-prolyl-tRNA at the ribosomal P-site reacts poorly with puromycin. Biochem. Biophys. Res. Commun. **366**:1043–1047.
37. **Muto H, Nakatogawa H, Ito K.** 2006. Genetically encoded but nonpolypeptide prolyl-tRNA functions in the A site for SecM-mediated ribosomal stall. Mol. Cell **22**:545–552.
38. **Nakatogawa H, Murakami A, Ito K.** 2004. Control of SecA and SecM translation by protein secretion. Curr. Opin. Microbiol. **7**:145–150.
39. **Onouchi H, et al.** 2005. Nascent peptide-mediated translation elongation arrest coupled with mRNA degradation in the *CGS1* gene of *Arabidopsis*. Genes Dev. **19**:1799–1810.
40. **Onoue N, et al.** 2011. *S*-Adenosyl-L-methionine induces compaction of nascent peptide chain inside the ribosomal exit tunnel upon translation arrest in the Arabidopsis *CGS1* gene. J. Biol. Chem. **286**:14903–14912.
41. **Pavesi A, Conterio F, Bolchi A, Dieci G, Ottonello S.** 1994. Identification of new eukaryotic tRNA genes in genomic DNA databases by a multistep weight matrix analysis of transcriptional control regions. Nucleic Acids Res. **22**:1247–1256.
42. **Pitonzo D, Yang Z, Matsumura Y, Johnson AE, Skach WR.** 2009. Sequence-specific retention and regulated integration of a nascent membrane protein by the endoplasmic reticulum Sec61 translocon. Mol. Biol. Cell **20**:685–698.
43. **Ramu H, Mankin A, Vazquez-Laslop N.** 2009. Programmed drug-dependent ribosome stalling. Mol. Microbiol. **71**:811–824.
44. **Ramu H, et al.** 2011. Nascent peptide in the ribosome exit tunnel affects functional properties of the A-site of the peptidyl transferase center. Mol. Cell **41**:321–330.
45. **Raney A, Law GL, Mize GJ, Morris DR.** 2002. Regulated translation termination at the upstream open reading frame in *S*-adenosylmethionine decarboxylase mRNA. J. Biol. Chem. **277**:5988–5994.
46. **Sachs MS, Geballe AP.** 2006. Downstream control of upstream open reading frames. Genes Dev. **20**:915–921.
47. **Sachs MS, et al.** 2002. Toeprint analysis of the positioning of translational apparatus components at initiation and termination codons of fungal mRNAs. Methods **26**:105–114.
48. **Shantz LM, Pegg AE.** 1999. Translational regulation of ornithine decarboxylase and other enzymes of the polyamine pathway. Int. J. Biochem. Cell Biol. **31**:107–122.
49. **Spevak CC, Ivanov IP, Sachs MS.** 2010. Sequence requirements for ribosome stalling by the arginine attenuator peptide. J. Biol. Chem. **285**:40933–40942.
50. **Varshney U, Lee CP, RajBhandary UL.** 1991. Direct analysis of aminoacylation levels of tRNAs in vivo. Application to studying recognition of *Escherichia coli* initiator tRNA mutants by glutaminyl-tRNA synthetase. J. Biol. Chem. **266**:24712–24718.
51. **Vazquez-Laslop N, Mankin AS.** 2011. Picky nascent peptides do not talk to foreign ribosomes. Proc. Natl. Acad. Sci. U. S. A. **108**:5931–5932.
52. **Vazquez-Laslop N, Ramu H, Klepacki D, Kannan K, Mankin AS.** 2010. The key function of a conserved and modified rRNA residue in the ribosomal response to the nascent peptide. EMBO J. **29**:3108–3117.
53. **Wang Z, Fang P, Sachs MS.** 1998. The evolutionarily conserved eukaryotic arginine attenuator peptide regulates the movement of ribosomes that have translated it. Mol. Cell. Biol. **18**:7528–7536.
54. **Wang Z, Gaba A, Sachs MS.** 1999. A highly conserved mechanism of regulated ribosome stalling mediated by fungal arginine attenuator peptides that appears independent of the charging status of arginyl-tRNAs. J. Biol. Chem. **274**:37565–37574.
55. **Wang Z, Sachs MS.** 1997. Arginine-specific regulation mediated by the *Neurospora crassa arg-2* upstream open reading frame in a homologous, cell-free *in vitro* translation system. J. Biol. Chem. **272**:255–261.
56. **Wang Z, Sachs MS.** 1997. Ribosome stalling is responsible for arginine-specific translational attenuation in *Neurospora crassa*. Mol. Cell. Biol. **17**:4904–4913.
57. **Werner M, Feller A, Piérard A.** 1985. Nucleotide sequence of yeast gene *CPA1* encoding the small subunit of arginine-pathway carbamoylphosphate synthetase: homology of the deduced amino acid sequence to other glutamine amidotransferases. Eur. J. Biochem. **146**:371–381.
58. **Wohlgemuth I, Brenner S, Beringer M, Rodnina MV.** 2008. Modulation of the rate of peptidyl transfer on the ribosome by the nature of substrates. J. Biol. Chem. **283**:32229–32235.
59. **Woolhead CA, Johnson AE, Bernstein HD.** 2006. Translation arrest requires two-way communication between a nascent polypeptide and the ribosome. Mol. Cell **22**:587–598.
60. **Wu C, Amrani N, Jacobson A, Sachs MS.** 2007. The use of fungal in vitro systems for studying translational regulation. Methods Enzymol. **429**:203–225.
61. **Wu C, et al.** 2012. Arginine changes the conformation of the arginine attenuator peptide relative to the ribosome tunnel. J. Mol. Biol. **416**:518–533.
62. **Yanagitani K, Kimata Y, Kadokura H, Kohno K.** 2011. Translational pausing ensures membrane targeting and cytoplasmic splicing of XBP1u mRNA. Science **331**:586–589.
63. **Yap MN, Bernstein HD.** 2009. The plasticity of a translation arrest motif yields insights into nascent polypeptide recognition inside the ribosome tunnel. Mol. Cell **34**:201–211.